Optomechanical Conversion by Mechanical Turbines

Miloš Knežević[*] and Mark Warner

Cavendish Laboratory, University of Cambridge, Cambridge CB3 0HE, United Kingdom
(Received 24 June 2014; revised manuscript received 22 September 2014; published 30 October 2014)

Liquid-crystal elastomers are rubbers with liquid-crystal order. They contract along their nematic director when heated or illuminated. The shape changes are large and occur in a relatively narrow temperature interval or at low illumination around the nematic-isotropic transition. We present a conceptual design of a mechanical, turbine-based engine using photoactive liquid-crystal elastomers to extract mechanical work from light. Its efficiency is estimated to be 40%.

I. INTRODUCTION

We propose a mechanical turbine-based engine to harness the contractions of soft, photoresponsive solids with a large stroke. We thus take photoactive nematic liquid-crystal elastomers (LCEs) as our working material. Related engines have been proposed before, for instance, based on the bend response of strips of nematic photoglasses connecting two wheels [1,2]. In contrast, we proposed a two-wheel stretch engine [3] using a nematic photo LCE. The engine had analogies to that of Steinberg *et al.* who studied chemical-to-mechanical energy conversion [4]. Here, we extend the two-wheel approach of Ref. [3] to mechanical turbine-based engines (see Fig. 1) in order to get a much higher conversion of light to mechanical work than in that paper. There is a similarity to a turbine that converted chemical to mechanical energy [5]. Here we analyze the mechanics and losses involved in such turbines. Modeling the geometrical and material parameters of this turbine-based engine, along with the known photoresponse of typical LCEs, suggests that its efficiency can be as high as 40%.

The basis of these two-wheel and turbine engines is that a nematic rubber strip passes, respectively, once around two wheels or multiply around spindles turning at the same rate. The strip reduces its natural length on heating or illumination during its transition around one wheel; since its length while on the wheel is fixed, the tension rises. On leaving the wheel, it physically contracts to its new equilibrium length, and, in thereby eliminating the tension that has arisen, does work on the wheels or spindles that are turning underneath it. A net work is done because the wheels are of different diameters or the spindles are tapered. This paper is about the mechanics, work cycle, and efficiency if spindles are used rather than wheels. With many passes around the spindles, the work cycle comes to resemble that of a turbine.

Classical elastomers are cross-linked polymer melts exhibiting liquid characteristics locally but are solidlike on a macroscopic scale. Incorporating molecular rods into the polymers of a simple elastomer leads to networks that combine orientational liquid-crystal order with the extreme stretchiness of rubber, that is, LCEs [6,7]. The shape of a monodomain LCE is very sensitive to the change of the nematic order parameter Q; network polymers are elongated by the directional order and mechanical shape change ensues. The order decreases on increasing the temperature, which manifests as a uniaxial contraction by a factor λ_m (< 1) of the elastomer along the nematic director [7]. The contraction is especially rapid in the vicinity of the transition temperature to the isotropic state. Analogous shape changes occur in photoelastomers in which photo-isomerizable dye molecules, rodlike in their *trans* ground state, are connected to the LCE structure [8,9]. Here, illumination causes the creation of bent-shaped *cis* isomers of the dye which act as impurities that reduce the nematic order, in turn, leading to a contraction of the photoelastomer. The presence of *cis* isomers raises the effective
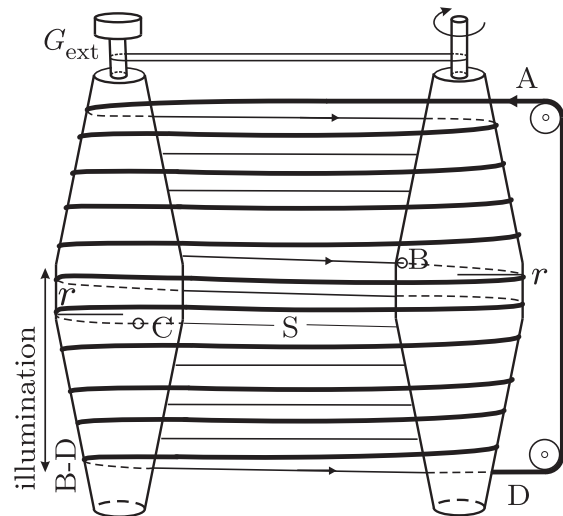

FIG. 1.   Schematic of an optomechanical turbine.

[*]mk684@cam.ac.uk

temperature of the photoelastomer from T to a pseudo-temperature $\tilde{T} > T$ which depends on the *cis* concentration and mimics the disorder as if it were induced thermally [8,10]. It is important to note that mechanical deformations of elastomers are reversible; that is, on removal of heat or light, recovery elongations by a factor of $1/\lambda_m$ occur. These elongations can be huge, up to 400% [11].

II. OPERATING PRINCIPLE

The optothermal cycle of our engine is shown in Fig. 2. For a nematic elastomer of shear modulus μ, the free energy per length of unstretched band F and the tension f depend on the stretch ratio (deformation gradient) λ [7]:

$$F(\lambda, T) = \frac{1}{2}\mu A_0 \left(P_{\parallel}\lambda^2 + \frac{2P_{\perp}}{\lambda} \right), \qquad (1)$$

$$\tilde{f} = \frac{f}{\mu A_0} = \frac{1}{\mu A_0}\left(\frac{\partial F}{\partial \lambda}\right)_T = \left(P_{\parallel}\lambda - \frac{P_{\perp}}{\lambda^2} \right), \qquad (2)$$

where A_0 is the cross-sectional area of the unstretched elastomer, and $\tilde{f} = f/(\mu A_0)$ is the tension reduced by the natural force scale in the problem. The modulus μ is temperature dependent. A simple, freely jointed rod (FJR) model quite accurately describes a wide range of LCEs [7,12] and, in particular, the development of photo-force [10]. In this model, the coefficients $P_{\parallel} = \ell_{\parallel}/\tilde{\ell}_{\parallel}$ and $P_{\perp} = \ell_{\perp}/\tilde{\ell}_{\perp}$ are the ratios of the effective step lengths of the network polymers at the reference temperature T and the current temperature $\tilde{T}$, respectively, parallel and perpendicular to the director. Before heating or illumination, the temperature is T; the extension factors λ are

FIG. 2. The optothermal cycle of the turbine-based engine. Reduced force $\tilde{f}$ against stretch λ. Upper curve, pseudotemperature $\tilde{T}$ (illuminated, isotropic state); bottom, lower T (nematic state). The grayed area represents the work done by the turbine-based engine having a finite number of extension and contraction steps (to be discussed in Sec. III). Dashed lines, two-wheel motor [3].

measured from the lengths in this initial state. The step lengths depend directly on the aspect ratio of the units of the polymer, but these cancel in the ratios P. These ratios depend on the nematic order parameters $Q(T)$ and $\tilde{Q} = Q(\tilde{T})$ in a simple way in the FJR model:

$$P_{\parallel} = (1 + 2Q)/(1 + 2\tilde{Q}) \quad \text{and} \quad P_{\perp} = (1 - Q)/(1 - \tilde{Q}). \qquad (3)$$

Note that the aspect ratio of the polymer units also contributes to the order Q. Along A → B, the current temperature is actually $\tilde{T} = T$ (nothing has changed) and $P_{\parallel} = 1$ and $P_{\perp} = 1$ trivially since $\tilde{Q} = Q$. The illuminated state C → D, with an elevated $\tilde{T} > T$, is isotropic with $\tilde{Q} \approx 0$ and the parameters are $P_{\parallel} = (1 + 2Q) > 1$ and $P_{\perp} = (1 - Q) < 1$.

A free elastomer has $\tilde{f} = 0$ in either the force-free state D with temperature $\tilde{T}$ or A with temperature T. Changing from the reference temperature T to $\tilde{T}$ and setting $\tilde{f} = 0$ in Eq. (2) then gives a contraction $\lambda_m = (P_{\perp}/P_{\parallel})^{1/3}$ of its natural length along its director [7]. Thus, $\lambda_m = [(1 - Q)/(1 + 2Q)]^{1/3}$. The large change between $\lambda = \lambda_m$ and $\lambda = 1$ is what makes LCEs promising working materials. We henceforth describe optical response, thermal response being entirely analogous. To realize a continu-ously operating engine, we subject the elastomer to a cyclical process through states A-B-C-D-A by changing the force and illumination.

It is easy to see from Fig. 2 that the net work delivered by the engine, per unit length of its LCE working material in its initial but unstretched state at T, as it is taken around the cycle, is

$$\begin{aligned} W &= W_{\text{CD}} - W_{\text{AB}} \\ &= \mu A_0 \left(\int_{\lambda_m}^{\lambda_h} \tilde{f}(\lambda; \tilde{T})d\lambda - \int_{1}^{\lambda_h} \tilde{f}(\lambda; T)d\lambda \right) \\ &\equiv \mu A_0 (I_1 - I_2) \\ &= F(\lambda_h, \tilde{T}) - F(\lambda_h, T) + \frac{3}{2}\mu A_0 (1 - (P_{\parallel}P_{\perp}^2)^{1/3}), \qquad (4) \end{aligned}$$

where the $\int \tilde{f}(\lambda; T)d\lambda$ are reduced force integrals. W is similar in form to the work done in the various gaseous p-V cycles. We assume the moduli are comparable, $\mu(T) \approx \mu(\tilde{T})$. Notice that the work W delivered is greater than the difference established in the free energies per length of band in its unstretched state at C and B by a (positive) term $\frac{3}{2}\mu A_0[1 - (P_{\parallel}P_{\perp}^2)^{1/3}]$ that arises during the cycle due to heat absorption.

One already sees from Fig. 2 that the prestretch λ_h imposed before illumination enhances work output con-siderably, just as a higher compression ratio improves
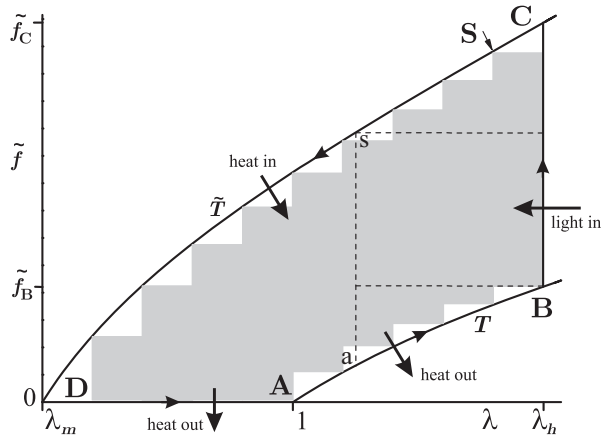
conventional engines. Further, taking a turbine allows one to extend the cycle to zero force (at a contraction equal to the natural illuminated length, λ_m), which is impossible in two-wheel stretch engines [3]; see cycle a-B-C-s-a in Fig. 2. However, for a soft solid, formidable problems exist in realizing the above W. These include sliding and the consequential frictional losses when finite tension differences in soft solids exist across the engine. The remainder of this paper is concerned with overcoming these problems to get close to the above W by using the turbine of Fig. 1. We will need to generalize the classical pulley result of Euler [13] to highly extensible belts.

The energy input per unit length of unstretched elastomer in the illumination process B-C is $\varepsilon n_{\mathrm{dye}} A_0$, with ε the appropriate photon energy and n_{dye} the number density of dye molecules. For our model of an isotropic elastomer, the internal energy is a function of temperature only and is unchanging along an isotherm [14]. Thus, the heat input per unit length of unstretched elastomer during the isothermal process C-D equals the work done W_{CD}. The efficiency is the ratio of the work done to the optical energy plus heat invested per cycle:

$$\eta = \frac{W_{\mathrm{CD}} - W_{\mathrm{AB}}}{W_{\mathrm{CD}} + \varepsilon n_{\mathrm{dye}} A_0} = \left(1 - \frac{I_2}{I_1}\right) \Big/ \left(1 + \frac{\varepsilon n_{\mathrm{dye}}}{\mu} \frac{1}{I_1}\right), \quad (5)$$

where I_1 and I_2 are the reduced force integrals in Eq. (4) and depend on the order along the isotherms T and $\tilde{T}$. From Eq. (2), they are clearly just the free-energy changes per length of band in its unstretched state (reduced by μA_0) between the relevant λ's, and involve the Q and $\tilde{Q}$ through the explicit expressions (3) for the $P(Q)$'s.

Since $I_1 > I_2$, the efficiency is always $0 < \eta < 1$. The ratio of material constants has been estimated as $\varepsilon n_{\mathrm{dye}}/\mu \approx 2$ [3,15]. Thus, the efficiency is determined by the value of the order parameter Q and the value of the prestretch λ_h. As an example, we take a modest value for the dark-state order $Q = 0.5$, which would yield $\lambda_m = 0.63$ or, equivalently, an elongation $1/\lambda_m = 1.58$ on recovering the nematic state from the isotropic, illuminated state. In fact, much greater elongations of approximately 4 are known. With $Q = 0.5$ and $\lambda_h = 3\lambda_m$, one obtains $\eta \approx 40\%$. We discuss dynamics and the influence on η at the end.

We now follow the mechanical-thermal cycle in detail. A closed band of photo LCE is wound around the pair of spindles of Fig. 1, the tops of which are rigidly coupled by a loop of inextensible wire, thus, ensuring they have equal angular velocities. The spindles have slightly tilted axes which enable the elastomer to spontaneously follow a helical path down the spindles as they rotate. The horizontal cross section of the spindles can be approximated by circles, the radii of which grow from the top to attain a largest value (r) at the middle section of the spindle, after which they then decrease.

Initially, a free elastomer belt in the nematic reference state A at temperature T comes onto the upper part of the spindles with $\lambda = 1$ and, hence, $f = 0$. Isothermally, it passes helically from smaller to larger spindle radii, extending at each pass by a fraction equal to the ratio of the radii which material conservation requires as discussed later. It suffers multiple-step extension during the process A-B in Fig. 2. State B achieved when the belt enters the cylindrical section of the spindle with the largest radius r (Fig. 1) has the highest (pre)stretch $\lambda = \lambda_h$ and has force $f = f_{\mathrm{B}}$. When in this region of radius r, the elastomer is illuminated and assumed to reach $\tilde{T}$ before it leaves the region; the extent of this region of the spindle is determined in part by dynamics since light absorption should proceed long enough to give sufficient dye conversion to attain the isotropic state before the band starts the contraction part of the cycle. Along the B-C path, the process is isometric ($\lambda = \lambda_h$, an assumption of no slip along the B-C path). At the point C, the force takes the highest value in the cycle f_{C}, and the elastomer is in the isotropic state. After passing the region of maximum radius r, the elastomer spirals down the lower part of the spindles, $\mathrm{C} \rightarrow \mathrm{D}$. It moves now repeatedly from larger to smaller radii, contracting at each pass by the ratio of the radii. It releases its elastic energy as work done on the spindles; in the final state D, the stretch reaches the minimum value $\lambda = \lambda_m$, the natural length of elastomer at $\tilde{T}$. To remain with $\tilde{T}$ along the C-D path, because of $cis \rightarrow trans$ backreaction one must continue some level of illumination. Equally, to remain isothermal, one needs external heat since entropy rises in a contracting elastomer. (In practice, much of this heat input can come directly or indirectly from the optical source: Photons have energy in the range 2 eV, which is equivalent to $80 k_{\mathrm{B}} T$ for $T \sim 300$ K; that is, large energies per absorption are available from quantum efficiencies of less than 100% in the $trans$ to cis transition. Equally, cis to $trans$ backreactions yield energies per dye molecule that are large on the thermal energy scale and are spread over the network molecules.) Finally, on removal of illumination, at zero force the elastomer gradually recovers and elongates from λ_m and $\tilde{T}$ to $\lambda = 1$ and T (D-A of the cycle). The engine converts into mechanical work part of the optical energy elevating the elastomer to the effective temperature $\tilde{T}$. Work is extracted by turning one spindle (the left in Fig. 1) against the external torque, G_{ext}.

III. FRICTIONAL LOSSES

The useful work done per cycle is less than that of Eq. (4) because of sliding friction. We analyze each pass of the elastomer around a spindle, considering differences in the tensions f_1 and f_2 of the incoming and outgoing sections; see Fig. 3(a).

Classically [13], there is an exponential increase of tension along a belt passing around a wheel [see Fig. 3(a) where tension increases from f_1 to f_2 over parts of $x = 0$
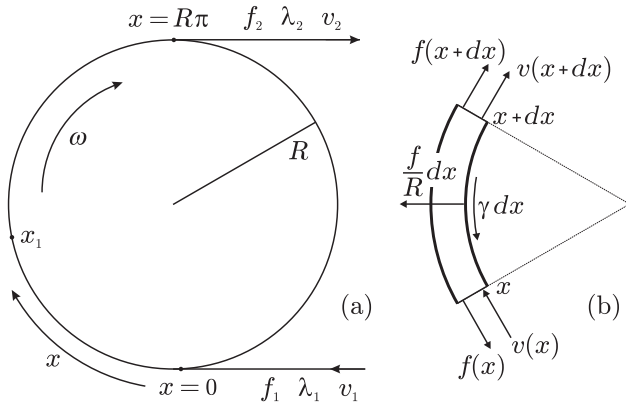
FIG. 3. (a) A spindle with a belt around it with a tension varying with position x around its circumference. (b) An expanded view of a short section of belt at $(x, x + dx)$ with a radial force and a frictional shear force acting on the belt.

to $x = \pi R$]. Since the surface is curved, there is an inward force per unit length on the spindle from the belt of f/R; see Fig. 3(b). If the surface is rough, the normal force gives a frictional shear force (per unit length on the circumference) of $\gamma \propto f/R$. The net shear force γdx on an element dx balances the difference in tangential forces $f(x+dx) - f(x) = (df/dx)dx$ across the element. Clearly, $\frac{df}{dx} = \gamma \propto f/R$ gives an exponential increase in $f(x)$. There is an obvious limitation to the classical analysis that is important in soft solids where substantial stretch λ must accompany increasing f: The belt has to slide on the spindle to extend so that f increases with x. It cannot translate with the circumferential speed $v = \omega R$ for all its contact length with the spindle but rather travel faster. Changing strain implies changing stored elastic energy. Sliding implies frictional losses during the transmission of power.

Figure 3(a) assigns a $\lambda(x)$ corresponding to an $f(x)$. In particular $\lambda = \lambda_1$ for the belt incoming onto the spindle, and $\lambda = \lambda_2$ when it emerges with f_2. Let the temperature be constant along the belt in contact with the spindle; then an increase of tension $f_2 > f_1$ implies $\lambda_2 > \lambda_1$. Soft solids are essentially incompressible under extension; hence, material conservation dictates volume conservation. The sectional area $A = A_0/\lambda$ must diminish as the belt extends by λ. The volume flux of the belt onto the spindle is $v_1 A = v_1 A_0/\lambda_1$ and must be matched by $v(x)A_0/\lambda(x)$ at a general point. Dividing through by A_0 gives

$$v_1/\lambda_1 = v(x)/\lambda(x) = v_2/\lambda_2, \tag{6}$$

which is the length of band per unit time passing, were it to be in its unstretched state. This flux of the length of the band is equivalent to $\omega R/\lambda_1$ when the band is not sliding. Since the final stretch is greater than the initial $\lambda_2 > \lambda_1$, it follows $v_2 > v_1$; the belt starts going faster than the spindle. There is sliding friction. Neglecting inertia [16], we get

$$\frac{df}{dx} = \mu_k \frac{f}{R}, \tag{7}$$

where μ_k is the coefficient of kinetic (sliding) friction giving $\gamma = \mu_k f/R$. Since $f_2 > f_1$, friction inhibits sliding in the $+x$ direction. Solving Eq. (7) gives

$$f(x) = f_2 \exp\left[\frac{\mu_k}{R}(x - \pi R)\right], \tag{8}$$

which differs from the classical result in its use of kinetic friction coefficient μ_k, and the passage of energy to friction and to elastic potential. The tension varies from $f = f_2$ at $x = \pi R$ down to $f = f_1$ at an $x = x_1$ given by

$$x_1 = R\left[\pi - \frac{1}{\mu_k}\ln\left(\frac{f_2}{f_1}\right)\right]. \tag{9}$$

In the initial section $(0, x_1)$, the tension retains its incoming value $f = f_1$. It is gradients df/dx that transfer force (torque) to the spindle in the region $(x_1, \pi R)$. There is a region $(0, x_1)$ without torque if $x_1 > 0$, that is, if $f_2 < f_1 e^{\mu_k \pi}$.

The power delivered to the spindle in one step of the A-B path of Fig. 2 with $f_2 > f_1$ and the spindle turning clockwise [see Fig. 3(a)] is the speed of its surface v_1 times the force exerted on it:

$$P_w = v_1 \int_{x_1}^{\pi R} dx \mu_k \frac{f(x)}{R} = v_1 \int_{x_1}^{\pi R} dx \frac{df}{dx} = v_1(f_2 - f_1). \tag{10}$$

The term $-v_1 f_1$ is the power given by the spindle to the incoming band. The power $v_1 f_2$ is the portion of the power $v_2 f_2$ delivered by the more tense band that actually finds its way to the spindle. Thus, all the useful power is delivered via the region that is slipping. When the band slips as soon as it makes contact with the wheel, slip is complete and $x_1 = 0$ in Eq. (9); then $f_2 = f_1 e^{\mu_k \pi}$ takes its maximal value, as does P_w in Eq. (10); $P_w = v_1 f_1(e^{\mu_k \pi} - 1)$.

The power lost to friction in a step of the A-B path is from the forces $(df/dx)dx$ acting on elements dx moving at speeds $v(x) - v_1$ relative to the elements:

$$P_f = \int_{x_1}^{\pi R} dx \frac{df}{dx}[v(x) - v_1], \tag{11}$$

with x_1 given by Eq. (9). The v_1 part is trivially $-v_1(f_2 - f_1)$, Eq. (10). The first term integrates by parts to $(f_2 v_2 - f_1 v_1) - \int_{x_1}^{\pi R} dx f(x) dv(x)/dx$. The latter part has $dv/dx = (v_1/\lambda_1)(d\lambda/dx)$ and becomes

$$-\frac{v_1}{\lambda_1}\int_{x_1}^{\pi R} dx f(x) \frac{d\lambda}{dx} = -\frac{v_1}{\lambda_1}\int_{\lambda_1}^{\lambda_2} d\lambda f(\lambda)$$

$$= -\frac{v_1}{\lambda_1}[F(\lambda_2, T) - F(\lambda_1, T)], \tag{12}$$

where we used Eq. (2) with $P_\parallel = P_\perp = 1$, since the elastomer is at T. Overall, the power lost to friction is

$$P_f = f_2(v_2 - v_1) - \frac{v_1}{\lambda_1}[F(\lambda_2, T) - F(\lambda_1, T)], \quad (13)$$

and does not involve the friction coefficient μ_k unless slippage is complete ($x_1 = 0$). In the process A-B of the engine, $\lambda_2 > \lambda_1$ is realized by moving the elastomer belt in each pass from a spindle surface of a smaller radius r_1 to a surface of a larger radius r_2. The velocities are $v_1 = \omega r_1$ and $v_2 = \omega r_2$. Then using Eq. (6), one gets $\lambda_2/\lambda_1 = r_2/r_1 > 1$, as required.

In process C-D, in each turn around a spindle the isotropic elastomer with $\tilde{T}$ goes from a larger to a smaller radius, $r_1 > r_2$ leading to $v_1 > v_2$ and $\lambda_1 > \lambda_2$ since $\lambda_2/\lambda_1 = r_2/r_1 < 1$. Hence, the band goes from a higher to lower force, $f_1 > f_2$; see Fig. 3(a). Note that the spindle's direction of turn is fixed in the clockwise direction by the engine operation as a whole, independent of the relative size of the forces. As before, there is an x_1 with no slip for $x < x_1$, while slippage occurs for x in the range $(x_1, \pi R)$. Repeating the above, the power delivered and the frictional power lost are

$$P_w = v_1(f_2 - f_1) < 0, \quad (14)$$

$$P_f = f_2(v_2 - v_1) + \frac{v_1}{\lambda_1}[F(\lambda_1, \tilde{T}) - F(\lambda_2, \tilde{T})]. \quad (15)$$

It remains for us to analyze the elastomer belt going around surfaces of radius r in the process B-C. Now the elastomer at force f_B and temperature T comes on the spindle where the illumination begins; see Fig. 1. In Fig. 3(a), we now have $f_1 = f_B$ and $\lambda_1 = \lambda_h$. We assume that the change T to $\tilde{T}$ occurs without slippage and is complete before the elastomer reaches the point C in Fig. 1, possibly after several passes around the central section. [Force rising from f_B to f_C without slippage assumes $df/dx < \mu_s f/r$ where μ_s is the static friction coefficient. Elongation is fixed at $\lambda = \lambda_h$, and the variation of f with x is from the changing $P_\perp$ and $P_\parallel$ factors in expression (2) for f.] After x_1, slippage then occurs and the force drops from f_C to f_S [in Fig. 3(a) $f_2 = f_S$, $\lambda_2 = \lambda_S$]. The state S is marked in Figs. 1 and 2. The net power delivered to the spindles on transit of the cylindrical section with radius r is

$$P_w = \omega r(f_S - f_B). \quad (16)$$

For the frictional losses, expression (15) with the appropriate values of stretches, velocities, and forces is still applicable since process C-S is part of C-D.

Excluding the middle spindle section of radius r, the power delivered to the spindle in each extension step of the A-B path is given by expressions of the form (10) and is clearly positive as one expects if $f_2 > f_1$. However, the

total power delivered in the A-B path is actually negative (see Fig. 2) since the band emerges stretched from A-B. This is due to the fact that one must add the highly negative contribution $-\omega r f_B$ of Eq. (16) to the set of positive contributions of the form (10). Similarly, in the C-D path, the highly positive term $\omega r f_S$ of Eq. (16) is added to negative contributions (14), making the total power delivered in the C-D path positive since the elastomer contracts.

We now calculate the total power P_{nk} delivered to the spindles by the elastomer for an n-stage contraction process C-D and k-stage extension process A-B. When the engine runs at a constant velocity ω, the net torque acting on each of the spindles is zero. For simplicity, we shall neglect frictional forces at the bearings. Then one can express the balance of torques on the each spindle separately. Beside the torques produced by the elastomer, one should take into account the torques due to the inextensible wire which couples the spindles, and the external torque G_{ext} acting on the left spindle (see Fig. 1). In such a way, one obtains a pair of equations which enable one to determine G_{ext} and, thus, the useful power $P_{nk} = \omega G_{ext}$:

$$P_{nk} = \omega \sum_{i=1}^{n} f_{i+1}(r_i - r_{i+1}) - \omega \sum_{j=1}^{k} f'_{j+1}(r'_{j+1} - r'_j). \quad (17)$$

Here, f_{i+1} and f'_{j+1} are the forces in the ith step of the C-D process and in the jth step of the A-B process, respectively, while r_i and r'_j are the corresponding spindle radii. In particular, $f_2 \equiv f_S$ and $r_1 \equiv r$ (force f_1 would be $f_1 \equiv f_C$). Clearly, since $r_i > r_{i+1}$ for all i, the first sum on the right-hand side of Eq. (17) $P_n = \omega \sum_{i=1}^{n} f_{i+1}(r_i - r_{i+1})$ is positive. Similarly, we have $f'_{k+1} \equiv f_B$ and $r'_{k+1} \equiv r$ (force f_1' would be zero). On the other hand, $P_k = -\omega \sum_{j=1}^{k} f'_{j+1}(r'_{j+1} - r'_j)$ is negative since $r'_{j+1} > r'_j$.

Using relations (13) and (15), the useful power is

$$P_{nk} = \frac{\omega r}{\lambda_h} \sum_{i=1}^{n} [F(\lambda_i, \tilde{T}) - F(\lambda_{i+1}, \tilde{T})] - \sum_{i=1}^{n} P_{f,i}$$
$$- \frac{\omega r}{\lambda_h} \sum_{j=1}^{k} [F(\lambda'_{j+1}, T) - F(\lambda'_j, T)] - \sum_{j=1}^{k} P'_{f,j}$$
$$= \frac{\omega r}{\lambda_h} W - \sum_{i=1}^{n} P_{f,i} - \sum_{j=1}^{k} P'_{f,j}, \quad (18)$$

where λ_i and λ'_j are the stretches, and $P_{f,i}$ and $P'_{f,j}$ are the frictional power losses in the contraction and extension steps, respectively. We now sketch a geometrical interpretation of Eq. (18). The first term of the last line is the maximum useful mechanical power $P = W\omega r/\lambda_h$, with $\omega r/\lambda_h$ being the flux of unstretched length (6). The maximum mechanical work W done per unit length of

unstretched elastomer in one cycle is given by the area in the solid line A-B-C-D-A in Fig. 2. The useful work done per unit length of unstretched elastomer in one cycle $W_{nk} = P_{nk}/(\omega r/\lambda_h)$ is the gray shaded area enclosed in Fig. 2 (where for simplicity the change in radii in each contraction and extension step is taken to be the same; see comments below). Thus, the work done in one cycle to overcome friction during the contraction process is equal to the area of the white regions between the solid curve C-D and the gray shaded area (the corresponding frictional power losses are $\sum_{i=1}^{n} P_{f,i}$). Similarly, the area of regions between the gray shaded area and the solid curve A-B corresponds to the term $\sum_{j=1}^{k} P'_{f,j}$ of Eq. (18).

By contrast, the two-wheel cycle a-B-C-s-a dashed in Fig. 2 has larger frictional losses: the areas between the isotherms a-B and C-s and the horizontal dashed lines, respectively, above and below them are much larger relative to the enclosed area a-B-C-s-a (the maximum theoretical work). The inaccessibility of an $\tilde{f} = 0$ state means the enclosed area is smaller than the turbine's area, even though the same optical energy input to go from B to C is required, further underscoring the superior efficiency of a turbine.

Notice that the more steps n and k, the more useful work per cycle is done. We shall compare the power P corresponding to an infinite number of extension and contraction steps, with the power P_{nk} given by expression (17), and determine how many steps n and k one needs to achieve, say, $P_{nk}/P = 0.9$.

As an illustration, we take the change of radii in the contraction process C-D to be the same for each step and equal to $\Delta r = (r - r_{n+1})/n$, where r_{n+1} is the final radius in the contraction process. Similarly, for the extension process A-B, we take $\Delta r' = (r - r'_1)/k$, where r'_1 is the initial radius in the extension process. From relations (6), it follows: $r/\lambda_h = r_i/\lambda_i = r_{n+1}/\lambda_m$ and $r'_1/1 = r'_j/\lambda_j = r/\lambda_h$. Here we used the facts that the stretch that corresponds to the radius r_{n+1} is actually the natural stretch $\lambda_m = (P_\perp/P_\parallel)^{1/3}$, and that the stretch corresponding to radius r'_1 is $\lambda = 1$. The stretch steps in the contraction and extension processes are then $\Delta\lambda = \Delta r \lambda_h/r = (\lambda_h - \lambda_m)/n$ and $\Delta\lambda' = \Delta r' \lambda_h/r = (\lambda_h - 1)/k$, respectively. The choice $\Delta\lambda = \Delta\lambda'$ was made in Fig. 2 and cones taken in Fig. 1, but these restrictions are not necessary.

The powers P_{nk} and P can be expressed as

$$P_{nk} = \mu A_0 \frac{\omega r}{\lambda_h} \left[\Delta\lambda \sum_{i=1}^{n} \left(P_\parallel(\lambda_h - i\Delta\lambda) - \frac{P_\perp}{(\lambda_h - i\Delta\lambda)^2} \right) \right.$$

$$\left. - \Delta\lambda' \sum_{j=1}^{k} \left(1 + j\Delta\lambda' - \frac{1}{(1 + j\Delta\lambda')^2} \right) \right],$$

$$P = \mu A_0 \frac{\omega r}{\lambda_h} \left[\int_{\lambda_m}^{\lambda_h} d\lambda \left(P_\parallel \lambda - \frac{P_\perp}{\lambda^2} \right) - \int_1^{\lambda_h} d\lambda \left(\lambda - \frac{1}{\lambda^2} \right) \right].$$

$$(19)$$

Taking $Q = 0.5$ and $\lambda_h = 3\lambda_m$, one finds $P_{nk}/P = 0.9$ for $n = 15$, $k = 15$.

The maximum mechanical work done per unit length of unstretched elastomer in one cycle $W = P/(\omega r/\lambda_h)$ is given in Eq. (4). The simple integrals above at constant temperatures return us to the free energies in Eq. (2).

IV. CONCLUSIONS

In summary, the optical contraction of photo LCEs can be used to harness optical energy to generate mechanical energy. Our mechanical turbine-based engine utilizes more effectively the optothermal cycle than the two-wheel engine [3]. Soft, extensible photosolids deliver large amounts of work, but their extensions and contractions lead to sliding and, hence, concomitant frictional losses. We analyze such losses and calculate the fraction of work lost due to them.

That our proposed photoconversion method has moving parts gives it a disadvantage over conventional photovoltaics, though rubber is highly durable and tough—for instance, car tires survive long use in harsh, abrasive conditions. Another difficulty that could perhaps be solved by chemical design, is degradation from the effect of UV light. The role of dynamics when attempting to attain the above efficiencies also remains a question. As we note, the residence time in the isometric state B-C needs to be long enough that light penetrates deeply to convert the whole thickness of the band to the isotropic state. For intense beams, this requires a nonlinear bleaching wave (of light-induced dye conversion) to traverse the thickness [10] just as that part of the band leaves the section of the spindle with maximal radius r. Longer residence simply gives time for backreaction without mechanical work being delivered. Light energy is wasted, and the efficiency drops from the values emerging from the above analysis. Thus, light intensity, band thickness, residence in the isometric state, and rotational rate are all related aspects of the dynamics and need optimization by future studies.

[1] M. Yamada, M. Kondo, J. Mamiya, Y. Yu, M. Kinoshita, C. J. Barrett, and T. Ikeda, Photomobile polymer materials: Towards light-driven plastic motors, Angew. Chem., Int. Ed. **47,** 4986 (2008).

[2] Y. Geng, P. L. Almeida, S. N. Fernandes, C. Cheng, P. Palffy-Muhoray, and M. H. Godinho, A cellulose liquid

crystal motor: A steam engine of the second kind, Sci. Rep. **3,** 1028 (2013).

[3] M. Knežević and M. Warner, Optomechanical elastomeric engine, Phys. Rev. E **88,** 040501(R) (2013).

[4] I. Z. Steinberg, A. Oplatka, and A. Katchalsky, Mechano-chemical engines, Nature (London) **210,** 568 (1966).

[5] M. V. Sussman and A. Katchalsky, Mechanochemical tur-bine: A new power cycle, Science **167,** 45 (1970).

[6] P. G. de Gennes, Physique moleculaire—reflexions sur un type de polymeres nematiques, C.R. Seances Acad. Sci., Ser. B **281,** 101 (1975).

[7] M. Warner and E. M. Terentjev, *Liquid Crystal Elastomers* (Oxford University Press, Oxford, 2007).

[8] H. Finkelmann, E. Nishikawa, G. G. Pereira, and M. Warner, A new opto-mechanical effect in solids, Phys. Rev. Lett. **87,** 015501 (2001).

[9] P. M. Hogan, A. R. Tajbakhsh, and E. M. Terentjev, UV manipulation of order and macroscopic shape in nematic elastomers, Phys. Rev. E **65,** 041720 (2002).

[10] M. Knežević, M. Warner, M. Čopič, and A. Sánchez-Ferrer, Photodynamics of stress in clamped nematic elastomers, Phys. Rev. E **87,** 062503 (2013).

[11] A. R. Tajbakhsh and E. M. Terentjev, Spontaneous thermal expansion of nematic elastomers, Eur. Phys. J. E **6,** 181 (2001).

[12] H. Finkelmann, A. Greve, and M. Warner, The elastic anisotropy of nematic elastomers, Eur. Phys. J. E **5,** 281 (2001).

[13] M. L. Euler, Remarques sur l'effect du frottement dans l'equilibre, Mem. Acad. Sci. Berlin **18,** 265 (1769).

[14] L. R. G. Treloar, *The Physics of Rubber Elasticity* (Oxford University Press, Oxford, 2005).

[15] M. Knežević and M. Warner, Photoferroelectric solar to electrical conversion, Appl. Phys. Lett. **102,** 043902 (2013).

[16] M. S. Bechtel, S. Vohra, K. I. Jacob, and C. D. Carlson, The stretching and slipping of belts and fibers on pulleys, J. Appl. Mech. **67,** 197 (2000).